0.1 V0 Selection

0.1.1 General V0 Reconstruction

$\Lambda(\bar{\Lambda})$ and K_S^0 particles are electrically neutral, and cannot be directly detected, but must instead be reconstructed through detection of their decay products, or daughters. This process is illustrated in Figure 1, and the main cuts used are shown in Tables 1 and 2. In general, particles which are topologically reconstructed in this fashion are called V0 particles. The decay channel $\Lambda \rightarrow p\pi^-$ was used for the identification of Λ hyperons (and, similarly the charge-conjugate decay for the $\bar{\Lambda}$ identification), and K_S^0 $\rightarrow \pi^+\pi^-$ for the identification of K_S^0 mesons. The class AliFemtoV0TrackCutNSigmaFilter (which is an extension of AliFemtoV0TrackCut) is used to reconstruct the V0s.
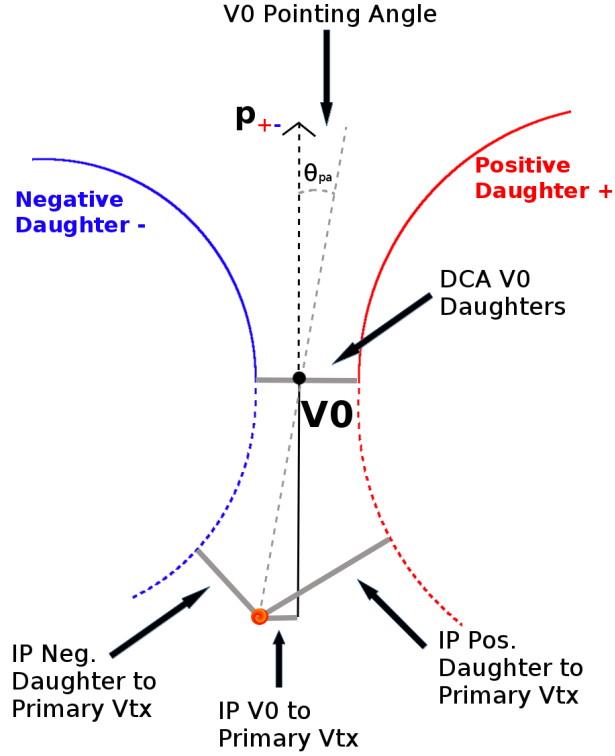

Fig. 1: V0 Reconstruction

To construct a V0 particle, the charged daughter tracks must first be found. Aside from typical kinematic and PID cuts (using TPC and TOF detectors), the daughter tracks are also exposed to a minimum cut on their impact parameter with respect to the primary vertex. The daughters of a V0 particle should not originate from the primary vertex, but rather from the decay vertex of the V0, hence the minimum cut imposition. The decay vertex of the V0 is assumed to be the point of closest approach between the daughter tracks. To help ensure quality, a maximum value cut is demanded on the distance-of-closest-approach between the daughters (DCA V0 Daughters). The positive and negative daughter tracks are combined to form the V0 candidate, the momentum of which is simply the sum of the momenta of the daughters (calculated at the DCA).

A minimum transverse momentum cut on the V0 candidate is introduced to reduce contamination from fake candidates. Opposite to that of the daughter tracks, the V0 candidate is exposed to a maximum cut on its impact parameter with respect to the primary vertex. In this case, we do want our V0 candidates to be primary, hence the maximum cut imposition. To further strengthen our selection of primary V0 candidates, we impose a selection on the pointing angle, θ_{pa}, between the V0 momentum and the vector pointing from the primary vertex to the secondary V0 decay vertex. We want the V0 candidate's momentum to point back to the primary decay vertex, and therefor a small θ_{pa}; we achieve this by appointing a

minimum value on $\cos(\theta_{\text{pa}})$ ("Cosine of pointing angle" in Tables 1 and 2).

On occasion, $\Lambda(\bar{\Lambda})$ particles are misidentified as K_S^0, and vice versa. To attempt to remove these contaminations without throwing away good candidates, we impose a set of misidentification cuts. The intent of these cuts is to judge whether a candidate is more likely a $\Lambda(\bar{\Lambda})$ or a K_S^0, and are implemented as described below. For a given V0, we calculate the mass assuming different identities (Λ, $\bar{\Lambda}$, K_S^0) of the candidate; the mass assuming K_S^0 hypothesis ($m_{\text{inv, }K_S^0\text{ hyp.}}$) is calculated assuming $\pi^+\pi^-$ daughters, the mass assuming Λ hypothesis ($m_{\text{inv, }\Lambda\text{ hyp.}}$) is calculated assuming $p\pi^-$ daughters, and the mass assuming $\bar{\Lambda}$ hypothesis ($m_{\text{inv, }\bar{\Lambda}\text{ hyp.}}$) is calculated assuming $\bar{p}\pi^+$ daughters. In addition to the notation just introduced, in the following, $m_{\text{PDG, }K_S^0}$ and $m_{\text{PDG, }\Lambda(\bar{\Lambda})}$ denote the particle masses of the K_S^0 and $\Lambda(\bar{\Lambda})$, respectively, as recorded by the Particle Data Group [?].

For $\Lambda(\bar{\Lambda})$ selection, a candidate is assumed to be misidentified and is rejected if all of the following criteria are satisfied:

1. $\left| m_{\text{inv, }K_S^0\text{ hyp.}} - m_{\text{PDG, }K_S^0} \right| < 9.0\,\text{MeV/}c^2$

2. The daughter particles pass daughter cuts intended for K_S^0 reconstruction

    (a) Λ selection

        i. p daughter passes π^+ cuts intended for K_S^0 reconstruction

        ii. π^- daughter passes π^- cuts intended for K_S^0 reconstruction.

    (b) $\bar{\Lambda}$ selection

        i. π^+ daughter passes π^+ cuts intended for K_S^0 reconstruction

        ii. $\bar{p}$ daughter passes π^- cuts intended for K_S^0 reconstruction.

3. $\left| m_{\text{inv, }K_S^0\text{ hyp.}} - m_{\text{PDG, }K_S^0} \right| < \left| m_{\text{inv, }\Lambda(\bar{\Lambda})\text{ hyp.}} - m_{\text{PDG, }\Lambda(\bar{\Lambda})} \right|$

Similarly, for K_S^0 selection, a candidate is rejected if all of the following criteria are satisfied for the Λ case, or for the $\bar{\Lambda}$ case:

1. $\left| m_{\text{inv, }\Lambda(\bar{\Lambda})\text{ hyp.}} - m_{\text{PDG, }\Lambda(\bar{\Lambda})} \right| < 9.0\,\text{MeV/}c^2$

2. The daughter particles pass daughter cuts intended for $\Lambda(\bar{\Lambda})$ reconstruction

    (a) π^+ daughter passes $p(\pi^+)$ daughter cut intended for $\Lambda(\bar{\Lambda})$ reconstruction

    (b) π^- daughter passes $\pi^-(\bar{p})$

3. $\left| m_{\text{inv, }\Lambda(\bar{\Lambda})\text{ hyp.}} - m_{\text{PDG, }\Lambda(\bar{\Lambda})} \right| < \left| m_{\text{inv, }K_S^0\text{ hyp.}} - m_{\text{PDG, }K_S^0} \right|$

At this stage, we have a collection of V0 candidates satisfying all of the aforementioned cuts. However, this collection is still polluted by fake V0s, for which the daughter particles happen to pass all of our cuts, but which do not actually originate from a V0. Although the two daughter particles appear to reconstruct a V0 candidate, they are lacking one critical requirement: the system invariant mass does not match that of our desired V0 species (these can be seen outside of the mass peaks in Fig. 4). Therefore, as our final single-particle cut, we require the invariant mass of the V0 candidate to fall within the mass peak of our desired species. Note, however, that some fake V0s still make it past this final cut, as their invariant mass also happens to fall without our acceptance window.

Occasionally, we encounter a situation where two V0 candidates share a common daughter. Not both of these candidates can be real V0s, and including both could introduce an artificial signal into our data. To avoid any auto-correlation effects, for each event, we impose a single-particle shared daughter cut on each collection of V0 candidates. This cut iterates through the V0 collection to ensure that no daughter is claimed by more than one V0 candidate. If a shared daughter is found between two V0 candidates, that candidate with a smaller DCA to primary vertex is kept while the other is excluded from the analysis. Note, this single-particle shared daughter cut is unique from the pair shared daughter cut discussed in Sec. **??**, the latter of which ensure there is no daughter sharing between the particles in a given pair.

The specific cuts used to reconstruct our $\Lambda(\bar{\Lambda})$ and K^0_S populations, along with plots showing the effect of the misidentification cuts, are shown in the following sections.

0.1.2 Λ Reconstruction

The following cuts, in addition to the misidentification and shared daughter cuts presented in Sec. 1.1, were used to select good $\Lambda(\bar{\Lambda})$ candidates:

Λ reconstruction		
$\lvert\eta\rvert$		< 0.8
p_T		> 0.4 GeV/c
$\lvert m_{\text{inv}} - m_{\text{PDG}}\rvert$		< 3.8 MeV
DCA to prim. vertex		< 0.5 cm
Cosine of pointing angle		> 0.9993
OnFlyStatus		false
Decay Length		< 60 cm
Shared Daughter Cut		true
Misidentification Cut		true
Daughter Cuts (π and p)		
$\lvert\eta\rvert$		< 0.8
Number of clusters in the TPC		> 80
Daughter status		kTPCrefit
DCA πp Daughters		< 0.4 cm
π-specific cuts		
p_T		> 0.16 GeV/c
DCA to prim vertex		> 0.3 cm
TPC and TOF Nσ Cuts		
$p < 0.5$ GeV/c		N$\sigma_{\text{TPC}} < 3$
$p > 0.5$ GeV/c	if TOF & TPC available	N$\sigma_{\text{TPC}} < 3$ & N$\sigma_{\text{TOF}} < 3$
	else	N$\sigma_{\text{TOF}} < 3$
p-specific cuts		
p_T		$> 0.5(p)$ [$0.3(\bar{p})$] GeV/c
DCA to prim vertex		> 0.1 cm
TPC and TOF Nσ Cuts		
$p < 0.8$ GeV/c		N$\sigma_{\text{TPC}} < 3$
$p > 0.8$ GeV/c	if TOF & TPC available	N$\sigma_{\text{TPC}} < 3$ & N$\sigma_{\text{TOF}} < 3$
	else	N$\sigma_{\text{TOF}} < 3$

Table 1: Λ reconstruction

Figure 2a shows the mass assuming K^0_S hypothesis for the Λ collection, i.e. assume the daughters are $\pi^+\pi^-$ instead of p$^+\pi^-$. Figure 2b is a similar plot, but is for the $\bar{\Lambda}$ collection, i.e. assume the daughters are $\pi^+\pi^-$ instead of $\pi^+\bar{p}^-$. The K^0_S contamination is visible, although not profound, in both, in the slight
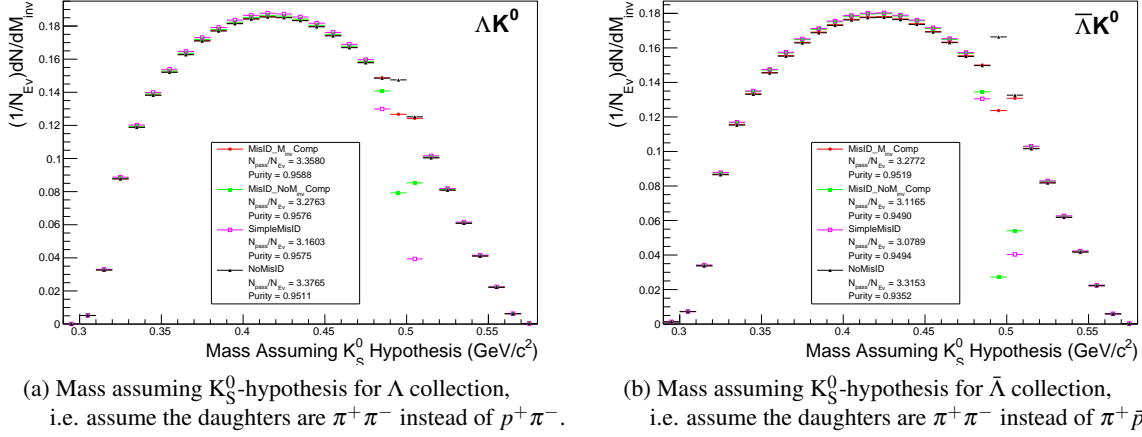
(a) Mass assuming K_S^0-hypothesis for Λ collection,
i.e. assume the daughters are $\pi^+\pi^-$ instead of $p^+\pi^-$.

(b) Mass assuming K_S^0-hypothesis for $\bar{\Lambda}$ collection,
i.e. assume the daughters are $\pi^+\pi^-$ instead of $\pi^+\bar{p}^-$.

Fig. 2: Mass assuming K_S^0-hypothesis for V0 candidates passing all Λ (2a) and $\bar{\Lambda}$ (2b) cuts. The "NoMisID" distribution (black triangles) uses the V0 finder without any attempt to remove misidentified K_S^0 The slight peak in the "NoMisID" distribution around $m_{inv} = 0.5$ GeV/c^2 contains misidentified K_S^0 particles in our $\Lambda(\bar{\Lambda})$ collection. "SimpleMisID" (pink squares) simply cuts out the entire peak, which throws away some good Λ and $\bar{\Lambda}$ particles. "MisID_NoM$_{inv}$Comp" (green squares) uses the misidentification cut outlined in the text, but does not utilize the final invariant mass comparison step. "MisID_M$_{inv}$Comp" (red circles) utilizes the full misidentification methods, and is currently used for this analysis. "N$_{pass}$/N$_{ev}$" is the total number of $\Lambda(\bar{\Lambda})$ particles found, normalized by the total number of events. The purity of the collection is also listed.

peaks around $m_{inv} = 0.497$ GeV/c^2. If one simply cuts out the entire peak, good Λ particles will be lost. Ideally, the Λ selection and K_S^0 misidentification cuts are selected such that the peak is removed from this plot while leaving the underlying distribution continuous. To attempt to remove these K_S^0 contaminations without throwing away good Λ and $\bar{\Lambda}$ particles, the misidentification cuts introduced in Sec. 1.1 were imposed.

0.1.3 K_S^0 *Reconstruction*

The following cuts, in addition to the misidentification and shared daughter cuts presented in Sec. 1.1, were used to select good K_S^0 candidates:

As can be seen in Figure 3, some misidentified Λ and $\bar{\Lambda}$ particles contaminate our K_S^0 sample. Figure 3a shows the mass assuming Λ-hypothesis for the K_S^0 collection, i.e. assume the daughters are $p^+\pi^-$ instead of $\pi^+\pi^-$. Figure 3b is similar, but shows the mass assuming $\bar{\Lambda}$-hypothesis for the collection, i.e. assume the daughters are $\pi^+\bar{p}^-$ instead of $\pi^+\pi^-$. The Λ contamination can be seen in 3a, and the $\bar{\Lambda}$ contamination in 3b, in the peaks around $m_{inv} = 1.115$ GeV/c^2. Additionally, the $\bar{\Lambda}$ contamination is visible in Figure 3a, and the Λ contamination visible in Figure 3b, in the region of excess around $1.65 < m_{inv} < 2.1$ GeV/c^2. This is confirmed as the number of misidentified Λ particles in the sharp peak of Figure 3a (misidentified $\bar{\Lambda}$ particles in the sharp peak of Figure 3b) approximately equals the excess found in the $1.65 < m_{inv} < 2.1$ GeV/c^2 region of Figure 3a (Figure 3b).

The peaks around $m_{inv} = 1.115$ GeV/c^2 in Figure 3 contain both misidentified $\Lambda(\bar{\Lambda})$ particles and good K_S^0. If one simply cuts out the entire peak, some good K_S^0 particles will be lost. Ideally, the K_S^0 selection and $\Lambda(\bar{\Lambda})$ misidentification cuts can be selected such that the peak is removed from this plot while leaving the underlying distribution continuous. To attempt to remove these Λ and $\bar{\Lambda}$ contaminations without throwing away good K_S^0 particles, the misidentification cuts introduced in Sec. 1.1 were imposed.

K_S^0 **reconstruction**	
$|\eta|$	< 0.8
p_T	> 0.2 GeV/c
$m_{PDG} - 13.677$ MeV $< m_{\text{inv}} < m_{PDG} + 2.0323$ MeV	
DCA to prim. vertex	< 0.3 cm
Cosine of pointing angle	> 0.9993
OnFlyStatus	false
Decay Length	< 30 cm
Shared Daughter Cut	true
Misidentification Cut	true
$\pi^{\pm}$ **Daughter Cuts**	
$|\eta|$	< 0.8
Number of clusters in TPC	> 80
Daughter Status	kTPCrefit
DCA $\pi^+\pi^-$ Daughters	< 0.3 cm
p_T	> 0.15 GeV/c
DCA to prim vertex	> 0.3 cm
TPC and TOF Nσ Cuts	

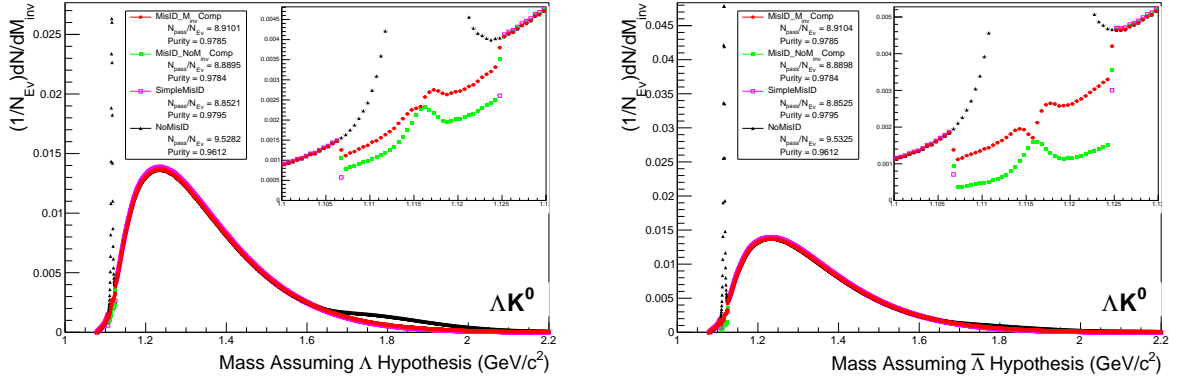| $p < 0.5$ GeV/c		N$\sigma_{\text{TPC}} < 3$
$p > 0.5$ GeV/c	if TOF & TPC available	N$\sigma_{\text{TPC}} < 3$ & N$\sigma_{\text{TOF}} < 3$
	else	N$\sigma_{\text{TOF}} < 3$

Table 2: K_S^0 reconstruction

(a) Mass assuming Λ-hypothesis for K_S^0 collection, i.e. assume the daughters are $p^+\pi^-$ instead of $\pi^+\pi^-$.

(b) Mass assuming $\bar{\Lambda}$-hypothesis for K_S^0 collection, i.e. assume the daughters are $\pi^+\bar{p}^-$ instead of $\pi^+\pi^-$.

Fig. 3: Mass assuming Λ-hypothesis (3a) and $\bar{\Lambda}$-hypothesis (3b) for K_S^0 collection. The "NoMisID" distribution (black triangles) uses the V0 finder without any attempt to remove misidentified Λ and $\bar{\Lambda}$. The peak in the "NoMisID" distribution around $m_{\text{inv}} = 1.115$ GeV/c^2 contains misidentified Λ (3a) and $\bar{\Lambda}$ (3b) particles in our K_S^0 collection. "SimpleMisID" (pink squares) simply cuts out the entire peak, which throws away some good K_S^0 particles. "MisID_NoM$_{\text{inv}}$Comp" (green squares) uses the misidentification cut outlined in the text, but does not utilize the final invariant mass comparison step. "MisID_M$_{\text{inv}}$Comp" (red circles) utilizes the full misidentification methods, and is currently used for this analysis. "N$_{\text{pass}}$/N$_{\text{ev}}$" is the total number of K_S^0 particles found, normalized by the total number of events. The purity of the collection is also listed. Also note, the relative excess of the "NoMisID" distribution around $1.65 < m_{\text{inv}} < 2.1$ GeV/c^2 shows misidentified $\bar{\Lambda}$ (3a) and Λ (3b) particles in our K_S^0 collection.

0.2 V0 Purity Estimation

In order to obtain a true and reliable signal, one must ensure good purity of the V0 collection. The purity of the collection is calculated as:

$$Purity = \frac{Signal}{Signal + Background} \tag{1}$$

To access both the signal and background, the invariant mass distribution (m_{inv}) of all V0 candidates must be constructed immediately before the final invariant mass cut, as shown in Fig. 4 for Λ, $\bar{\Lambda}$ and K_S^0 candidates in the 0-10% centrality bin. Fig. 4a presents the $p\pi^-$ invariant mass distribution showing the Λ peak, Fig. 4b presents the $\bar{p}\pi^+$ invariant mass distribution showing the $\bar{\Lambda}$ peak, and Fig. 4c presents the $\pi^+\pi^-$ invariant mass distribution showing the K_S^0 peak.

It is vital that this distribution be constructed immediately before the final m_{inv} cut, otherwise it would be impossible to estimate the background. These distributions are used to calculate the collections' purities (defined in Eq. 1). As shown in Figure 4, the background is fit (with a polynomial) outside of the peak region of interest to obtain an estimate for the background within the region. Within the m_{inv} cut limits, the background is assumed to be the region below the fit while the signal is that above the fit. The Λ and $\bar{\Lambda}$ purities were found to be $\approx 95\%$, and the K_S^0 purity was found to be $\approx 98\%$.

0.3 V0 Purity Background Estimation

As previously stated, the backgrounds in the m_{inv} distributions are modeled by a polynomial which is fit outside of the final cut region in an attempt to estimate the background within the cut region. As this estimate of the background under the mass peak is vital for our estimate of our V0 purity, it is important for us to ensure that our estimate is accurate. More specifically, it is necessary that we ensure the background is well described by a polynomial fit within the cut region.

To better understand our background, we studied V0 candidates reconstructed with daughters from different events. These mixed-event V0s certainly do not represent real, physical V0s (a single V0 cannot have daughters living in two different events!), but, rather, represent a large portion of the background creeping into our analysis.

The standard AliFemto framework is not equipped to handle this situation, as most are not interested in these fake-V0s. Therefore, we built a new class, AliFemtoV0PurityBgdEstimator, to handle our needs. In addition to finding fake-V0s using mixed-event daughters, we also used our new class to find real-V0s using same-event daughters. The purpose here was to compare our new class to the established V0 finder used in standard AliFemto analyses.

Figure 5 shows the results of our study. In the figures, the black points, marked "Data", correspond to V0s found using the standard V0-finder, and to the V0s used in my analyses. The red and blue points utilize our personal V0-finder (i.e. AliFemtoV0PurityBgdEstimator). The red points show real V0s reconstructed using same-event daughters, and the blue points show fake-V0s reconstructed using mixed-event daughters. Both the red and blue points have been scaled by different factors (listed in the legends) to nicely align all three data on a single plot.

Figure 5 shows that our personal V0-finder does a good, but not perfect, job of matching the shape of the m_{inv} plots obtained from the data. The scale factor listed in the legend reveals that we are only finding 1/3 - 1/2 of the V0s found by the standard V0-finder. These two points are not of concern, as our purpose here was to gain a sense of the broad shape of the background. It is revealed in Fig. 5, when studying the red and blue points, that the background distribution within the mass peak region is simply a smooth connection of the backgrounds outside of the cut region, as we assumed. Therefore, our method of fitting the background outside of the cut region, fitting with a smooth polynomial, and extrapolating to the cut
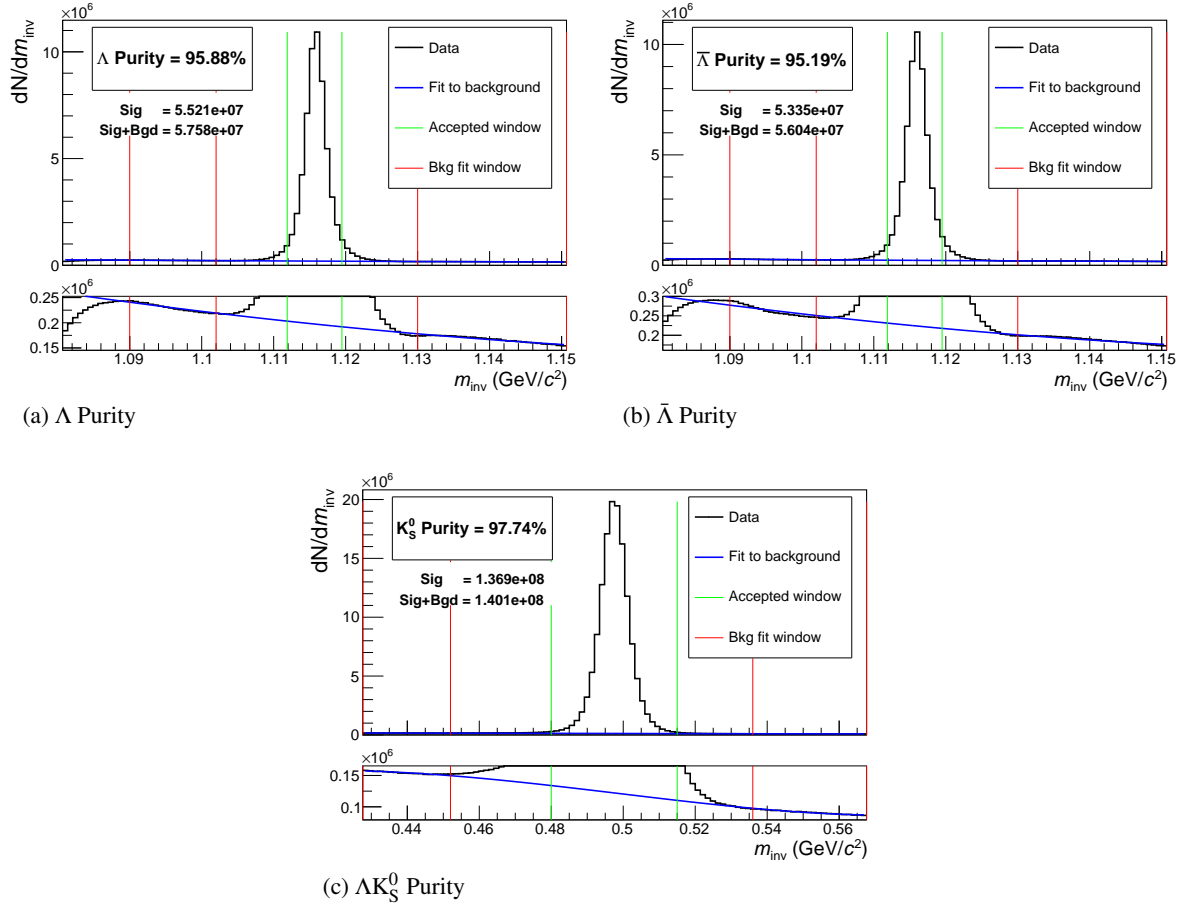
(a) Λ Purity

(b) $\bar{\Lambda}$ Purity

(c) ΛK_S^0 Purity

Fig. 4: Invariant mass (m_{inv}) distribution for all Λ (a), $\bar{\Lambda}$ (b), and K_S^0 (c) candidates immediately before the final invariant mass cut. The bottom figures are zoomed to show the background with fit. The vertical green lines represent the m_{inv} cuts used in the analyses, the red vertical lines delineate the regions over which the background was fit, and the blue line shows the background fit. These distributions are used to calculate the collection purities, Purity(Λ) $\approx$ Purity($\bar{\Lambda}$) $\approx$ 95%, and Purity(K_S^0) $\approx$ 98%.

region is justified.

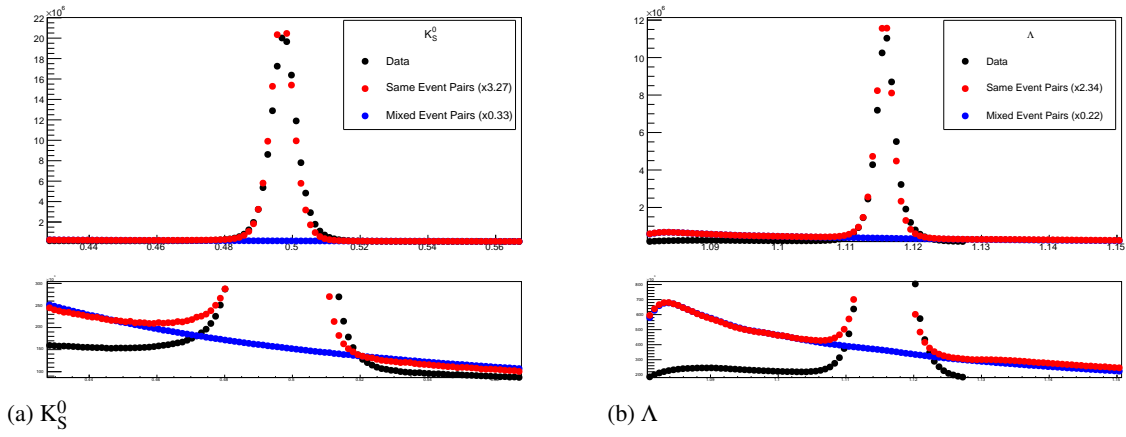(a) K_S^0 (b) Λ

Fig. 5: V0 Purity Background Estimation. The black points, marked "Data", correspond to real V0s found using the standard V0-finder (i.e. the V0s used in my analyses). The red points, marked "Same Event Pairs", show real V0s reconstructed with our personal V0-finder in AliFemtoV0PurityBgdEstimator. These data are scaled by a factor (listed in the legend) to match their *Signal + Background* value in the cut region with that of the data. The blue points, marked "Mixed Event Pairs", show fake-V0s reconstructed with our personal V0-finder using mixed-event daughters. The blue points are scaled by a factor (listed in the legend) to closely match the red points in the side-band region.